COVER SHEET

Paper Number: **2909**

Title: Nondestructive Evaluation of Adhesive Bonds via Ultrasonic Phase Measurements

Authors: Harold A. Haldren
Daniel F. Perey
William T. Yost
K. Elliott Cramer
Mool C. Gupta

(FIRST PAGE OF ARTICLE – align this to the top of page – leave space blank above ABSTRACT)

ABSTRACT

The use of advanced composites utilizing adhesively bonded structures offers advantages in weight and cost for both the aerospace and automotive industries. Conventional nondestructive evaluation (NDE) has proved unable to reliably detect weak bonds or bond deterioration during service life conditions. A new nondestructive technique for quantitatively measuring adhesive bond strength is demonstrated. In this paper, an ultrasonic technique employing constant frequency pulsed phased-locked loop (CFPPLL) circuitry to monitor the phase response of a bonded structure from change in thermal stress is discussed. Theoretical research suggests that the thermal response of a bonded interface relates well with the quality of the adhesive bond. In particular, the effective stiffness of the adhesive-adherent interface may be extracted from the thermal phase response of the structure. The sensitivity of the CFPPLL instrument allows detection of bond pathologies that have been previously difficult-to-detect. Theoretical results with this ultrasonic technique on single epoxy lap joint (SLJ) specimens are presented and discussed. This technique has the potential to advance the use of adhesive bonds – and by association, advanced composite structures – by providing a reliable method to measure adhesive bond strength, thus permitting more complex, lightweight, and safe designs.

INTRODUCTION

As aerospace and automotive technologies advance, so does the desire to use lightweight advanced composite structures such as carbon fiber reinforced polymers (CFRP). Bolting and riveting, widely used with metal-to-metal bonding, however, raise a series of specific problems with composites. Hence, adhesive bonding is a preferred method to join two composite materials. Means to monitor the bond's properties to

Harold A. Haldren, Dept. of Electrical and Computer Engineering, University of Virginia, NASA LaRC, 4 Langley Blvd., Bldg. 1230, MS231, Hampton, VA 23681
Daniel F. Perey, William T. Yost, K. Elliott Cramer, NASA LaRC, 4 Langley Blvd., Bldg. 1230, MS231, Hampton, VA 23681
Mool C. Gupta, Dept. of Electrical and Computer Engineering, University of Virginia, Thornton Hall, 351 McCormick Rd, Charlottesville, Virginia 22904-4743

transfer load (adhesive bond strength) ensure strength and stability of adhesively bonded structures. Consequently, a method to quantitatively determine the strength of an adhesive bond should be explored to ensure strength and stability of bonded structures.

Various nondestructive evaluation (NDE) techniques have been employed to characterize bonding defects, such as pores, delaminations, and complete disbonds; however, detecting weak or "kissing" bonds has proved extremely difficult via conventional NDE. To ensure adhesive bond quality, an NDE method must not only be sensitive to major adhesive layer defects, but it must also be able to measure small differences in interfacial degradation between the adhesive and adherent. Wider adoption of adhesive bonding in composite aerospace structures will likely be held back until a method is developed to quantitatively measure adhesion quality.

Much of the NDE research into adhesive bonding has focused on ultrasonic testing (UT), partially because acoustic waves can mechanically interrogate the bonded joint. However, the interfacial layer between adherent and adhesive is extremely thin in comparison to the wavelengths used in conventional UT. Additionally, poor adhesion will often not produce a measurable change in ultrasonic pulse amplitude, especially if the poor adhesion is not due to major defects such as voids and delaminations. Thus, these "kissing bonds", where the adhesive and adherent are in physical contact but little-to-no real physical attraction exists, have proved very difficult to detect via conventional UT. Consequently, researchers have looked to novel UT methods to characterize adhesive interfaces.

Several methods have been developed over the past decade or so that claim sensitivity to adhesive interface quality. Some of these methods observe frequency-domain characteristics of a reflected acoustic pulse in an attempt to measure interfacial properties. Linear [1] and modulated [2] angle beam ultrasonic spectroscopy (ABUS) measure interfacial quality by observing the shift in frequency minimum of the ultrasonic reflection coefficient for both normal incidence and oblique incidence waves. The characteristic frequency of the ultrasonic reflection coefficient, marking the transition between low and high frequency regions, was used by Nagy to measure interfacial properties for normal and transverse waves [3].

In addition to frequency-based methods, researchers have used ultrasonic signal phase to measure adhesion quality. In the study of dry contact interfaces, which are sometimes used to simulate kissing bonds, Królikowski and Szczepek used the pulse-echo overlap technique [4] to measure the phase of the reflection coefficient of an ultrasonic pulse [5]. They showed the measured phase shift for dry contacting surfaces of different roughness was sensitive to both the contact stiffness and fraction of real surface area contact. Recently, the phase of the ultrasonic reflection coefficient at an imperfect interface has been used to measure the quality of titanium diffusion bonding using double-sided and single-sided methods [6], [7]. In these phase measurements, it was shown that keeping the signal-to-noise ratio (SNR) high was crucial to ensuring the standard deviation of phase measurements was low enough to characterize a diffusion bond as good or bad.

While several of the mentioned methods have shown sensitivity to interfacial degradation, and thus adhesive bond strength, none have become ubiquitous adhesive bond strength measurement methods for various reasons. Conventional amplitude-based UT lacks the required sensitivity to measure kissing bonds, as the wavelengths generally used are very long in comparison to the interface layer. Also, many of the frequency-based UT methods require complex setup and processing that may only be

feasible in a laboratory setting. Finally, while phase-based techniques have shown promise in having high sensitivity to interfacial quality, they require a very high signal-to-noise ratio, which has been difficult to obtain with broadband ultrasonic pulses. Therefore, an ultrasonic NDE method utilizing signal phase to characterize adhesion quality is demonstrated in this work. This method utilizes a constant-frequency ultrasonic wave train, which allows for superior SNR in comparison to broadband pulses, as undesired frequencies can be filtered out of the measurement.

METHODS

Theory of Ultrasonic Wave Reflection from Imperfect Interfaces

Most of the ultrasonic methods evaluating adhesion quality use some variation of a distributed massless system or mass-spring system to mathematically model the adhesive-adherent interface. Massless spring boundary conditions were proposed by Tattersall in the early 1970s to model the "slackness" and frequency dependence of the observed ultrasonic reflection amplitude at an adhesive bonding interface [8]. Later, Baik and Thompson developed a more robust model for ultrasonic reflection at imperfect interfaces using a mass-spring system [9]. However, the mass contribution is assumed to be negligible for interfaces consisting of distributed thin cracks, reducing the mass-spring model to the massless spring model, which is often assumed for adhesive bonds without major inclusions or voids. The massless spring system can also be arrived at by looking at a tri-layer structure and assuming the acoustic impedance and thickness of the middle layer are much smaller than that of the exterior layers [10]. Additionally, Cantrell has shown that interfacial stiffness spring constants can be directly related to absolute adhesion strength for both alumina-epoxy [11] and carbon fiber-epoxy bonding [12]. Therefore, measuring interfacial stiffness is imperative for quantitatively measuring adhesion strength.

The normal-incidence ultrasonic displacement wave reflection coefficient from [8] for an imperfect interface modelled by a massless spring system can be written as

$$R = \frac{Z_1 - Z_2 + i\omega\left(\frac{Z_1 Z_2}{K}\right)}{Z_1 + Z_2 + i\omega\left(\frac{Z_1 Z_2}{K}\right)}, \tag{1}$$

where Z_i is the acoustic impedance of each respective medium, $\omega = 2\pi f$ is the angular frequency of the ultrasonic displacement wave, $i = \sqrt{-1}$ is the imaginary unit, and K is the interfacial spring stiffness constant. The interfacial stiffness constant, K, represents the quality of adhesion between the adhesive and adherent layers. For a perfect interface, the spring boundary becomes completely rigid, $K \to \infty$, and the reflection coefficient reverts to its standard form of

$$R = \frac{Z_1 - Z_2}{Z_1 + Z_2}. \tag{2}$$

For a complete disbond where the boundary of medium 1 becomes a free surface, which means the spring boundary becomes infinitely slack, $K \to 0$, and all incident energy is reflected with a reflection coefficient of $R = 1$. The differences between these

two extremes may be detectable via amplitude measurements, but to measure stiffness values with high resolution in between the extremes, other methods based on phase or frequency measurements must be used.

While Equation 1 shows the reflection coefficient from a single imperfect interface, a standard single-lap-joint (SLJ) consists of three layers and two potentially imperfect interfaces, complicating the model and ultrasonic measurement process. Consider a tri-layered structure representing a SLJ with Media 1, 2, and 3, as shown in Figure 1. In this setup for a SLJ with the same material used for the adherent on both sides of the bond-line, the acoustic impedance in Medium 1 will be the same as the acoustic impedance in Medium 3. Suppose an incident ultrasonic displacement wave with an amplitude of one for derivation simplicity has the form

$$u_i = e^{i\omega\left(t-\frac{x}{c_1}\right)}, \tag{3}$$

where $\omega = 2\pi f$ is the driving frequency of the wave, t is time, x is the distance into the structure, and c_1 is the ultrasonic velocity in the adherent, Medium 1.

At this point, the total reflection coefficient of the bonded structure with two imperfect interfaces can be derived via several different methods. The approach shown by [13] uses an infinite number of decaying reflections from within the adhesive layer contributing to the total reflection from the bonded structure. As it has already been derived for a similar structure, the infinite reflections approach to modeling ultrasonic reflection from a SLJ structure will be used. In [13], it is assumed that the adhesion quality or spring stiffness constant, K_i, is the same at each interface. In real adhesively bonded structures, that assumption may not be valid, as one interface could be contaminated while the other may not, so the spring constants will not be assumed equal here.

Assuming the two interfaces in the tri-layer structure are thin in comparison to the ultrasonic wavelength used, spring boundary conditions can be used for each interface. K_i for each of the two interfaces is defined in the same manner as [13]:

$$K_i = \frac{increase\ in\ stress\ on\ the\ media}{increase\ in\ separation\ between\ media} = \frac{\sigma_{K_i}}{\Delta u}. \tag{4}$$

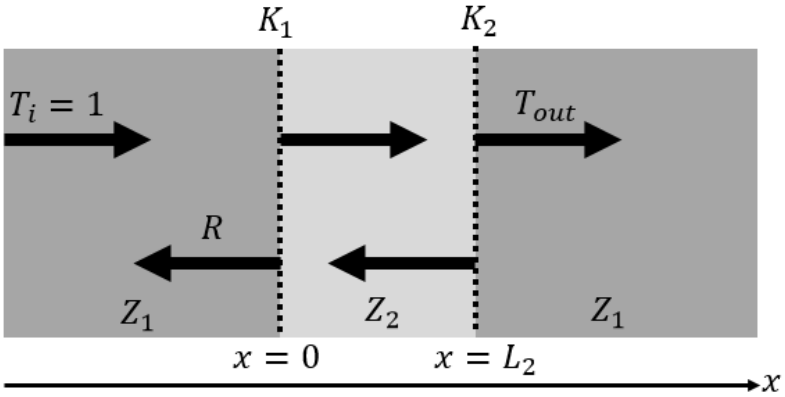

Figure 1. Tri-layer structure representing a SLJ

This definition of interfacial stiffness gives two boundary conditions for each interface. At each interface, there will be both an incident and reflected wave on the left side with a transmitted wave on the right side. Using the setup shown in Figure 1 where $x = 0$ at the first interface and $x = L_2$, the adhesive thickness, at the second interface, the four total boundary conditions can be written as,

$$\begin{aligned} \sigma_{K_1} &= K_1(u_1 - u_2), \\ \sigma_1 &= \sigma_2 = \sigma_{K_1}, \\ \sigma_{K_2} &= K_2(u_2 - u_3), \\ \sigma_2 &= \sigma_3 = \sigma_{K_2}. \end{aligned} \tag{5}$$

Solved for the general case of oblique incidence compressional waves by [14], the reflection and transmission coefficients for normal incidence waves using boundary conditions from Equation 5 can be seen in TABLE 1. Here, R_{ij} and T_{ij} are the reflection and transmission coefficients for an ultrasonic wave propagating from Medium i to Medium j. When calculating the total combined reflection from the tri-layer structure, there will be a contribution of reflection from the first interface and a summation of infinite decaying reflections off the second interface, as seen in Equation 6.

$$R = R_{12} + R_{sum} \tag{6}$$

To determine R_{sum}, consider individual reflections from the tri-layer structure. Figure 2 shows the reflection from the first interface and the first three reflections from the second interface. The infinite sum can be simplified by looking for common factors, as seen in Equation 7, where $k_2 = \omega/c_2$ is the wavenumber in Medium 2.

$$\begin{aligned} R_{sum} &= T_{12}T_{21}\mathrm{R}_{23}e^{2ik_2L_2}\left(1 + R_{23}R_{21}e^{2ik_2L_2} + \left(R_{23}R_{21}e^{2ik_2L_2}\right)^2 + \cdots\right) \\ &= T_{12}T_{21}R_{23}e^{2ik_2L_2}\sum_{n=0}^{\infty}\left(R_{23}R_{21}e^{2ik_2L_2}\right)^n = \frac{T_{12}T_{21}R_{23}e^{2ik_2L_2}}{1-R_{23}R_{21}e^{2ik_2L_2}}, \end{aligned} \tag{7}$$

TABLE 1: REFLECTION AND TRANSMISSION COEFFICIENTS AT EACH INTERFACE

	Reflection	*Transmission*
1-2 Interface	$R_{12} = \dfrac{Z_2 - Z_1 + i\omega\frac{Z_1Z_2}{K_1}}{Z_2 + Z_1 - i\omega\frac{Z_1Z_2}{K_1}}$	$T_{12} = \dfrac{2Z_1}{Z_2 + Z_1 - i\omega\frac{Z_1Z_2}{K_1}}$
2-1 Interface	$R_{21} = \dfrac{Z_1 - Z_2 + i\omega\frac{Z_1Z_2}{K_1}}{Z_2 + Z_1 - i\omega\frac{Z_1Z_2}{K_1}}$	$T_{21} = \dfrac{2Z_2}{Z_2 + Z_1 - i\omega\frac{Z_1Z_2}{K_1}}$
2-3 Interface	$R_{23} = \dfrac{Z_1 - Z_2 + i\omega\frac{Z_1Z_2}{K_2}}{Z_1 + Z_2 - i\omega\frac{Z_1Z_2}{K_2}}$	N/A

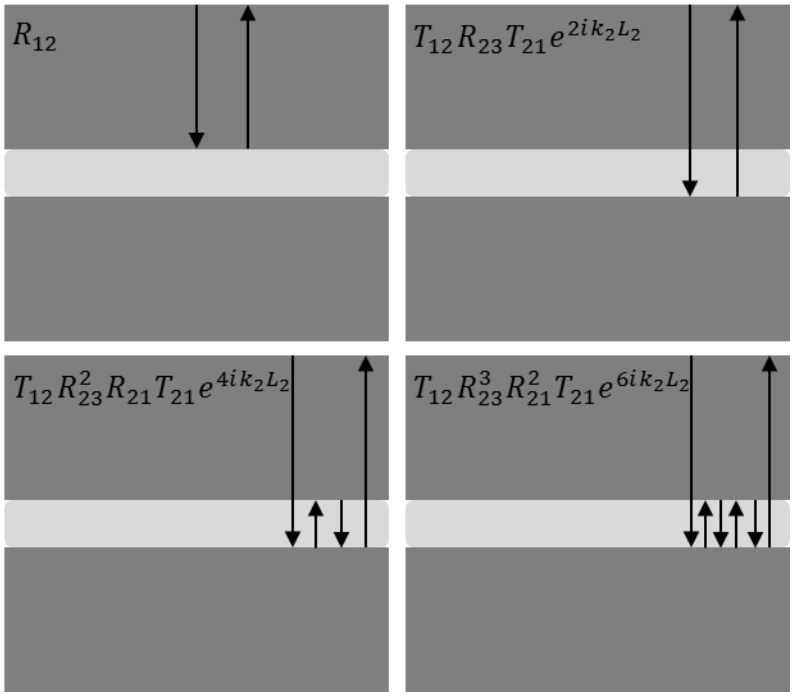

Figure 2: Individual reflections from tri-layer structure

Interfacial Stiffness Measurement Approach

By applying small temperature change to a bonded joint, thermal expansion will change the path length of sound through both the adherent and adhesive. This change in path length with temperature can be seen in the phase shift of an ultrasonic wave. Depending on the quality of the adhesive interfaces, different ultrasonic intensities will be reflected or transmitted at the interfaces, resulting in a change in the number of reflections from the adhesive layer contributing significantly to the phase shift of the total ultrasonic reflection signal. For instance, a good or stiff interface will tend to allow a higher intensity of ultrasound to transmit into the adhesive, increasing the total phase shift due to the adhesive layer.

If the applied temperature change is small, the interfacial stiffness constants can be considered approximately constant[2] and should be measureable by observing the phase shift in an ultrasonic wave with respect to temperature change. The phase shift of the reflection coefficient from a SLJ with respect to temperature will be influenced by changes in the top adherent, the transducer itself, and the two imperfect interfaces mixed with the adhesive layer, leading to an equation written

$$\Delta\phi_R|_{f=f_0} = \Delta T(\Delta\phi_{adherent} + \Delta\phi_{transducer} + \Delta\phi_{adhesive}). \quad (8)$$

[2] In [11], it was shown that the true adhesive strength for alumina-epoxy bonds can be expressed, $\sigma_{true} = P_{bond}\sigma_{max}$, where P_{bond} is the probably a given bond is intact at a particular temperature. Additionally, the normal interfacial stiffness can be directly related to true adhesive strength by $\sigma_{true} = \left(\frac{F_{max}}{k}\right)K_N$. Using $P_{bond} = (1 - P_{n\geq m})$, where $P_{n\geq m} = e^{-\frac{hv(1+m)}{k_BT}}\left(1 - e^{-\frac{hv}{k_BT}}\right)^{-2}$, results in only a -0.00035% drop in σ_{true} and K_N as temperature increases from $20°C$ to $25°C$.

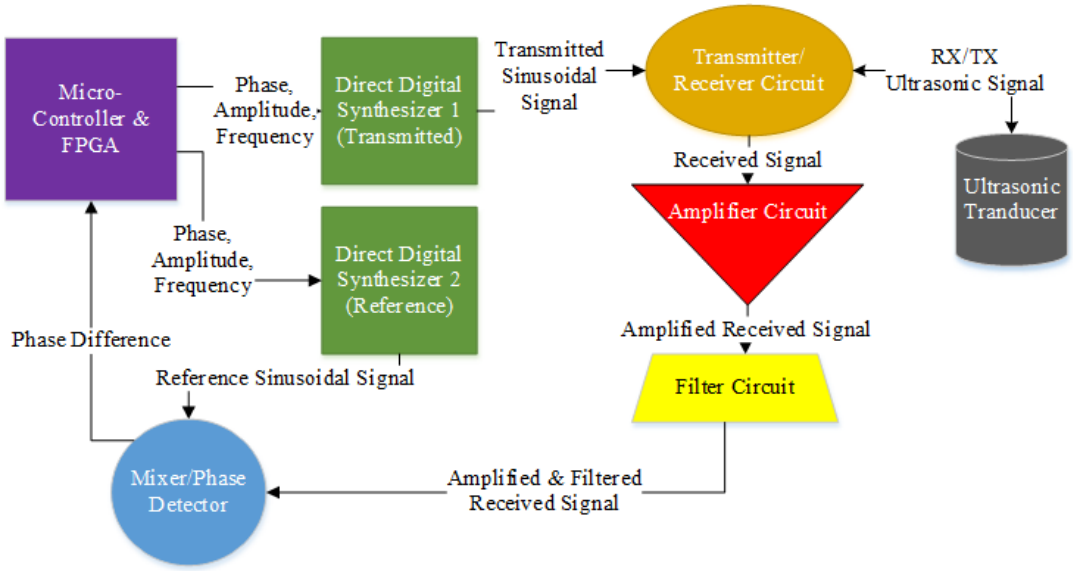

Figure 3: Block diagram of CFPPLL ultrasonic phase measurement system

EXPERIMENTAL

CFPPLL-Based Ultrasonic Phase Measurement Method

Previously, researchers have used a high frequency pulse of ultrasound to make phase versus frequency measurements [6], [7]. In this way, the phase versus frequency information can be obtained from a single received pulse from Fourier analysis. It was shown that controlling the signal to noise ratio of these experiments was extremely important in reducing the standard deviation of true phase measurements from imperfect interfaces. With broadband pulses, however, reducing noise beyond a certain point can be difficult. Accordingly, a method has been developed that can measure the absolute phase from a bonded joint at a constant frequency, enabling very high phase resolution and low noise sensitivity due to narrowband filtering.

The constant-frequency ultrasonic phase measurement method developed here is based on the constant frequency pulse phase-locked loop (CFPPLL) device originally developed by [15] to measure ultrasonic velocity. The current measurement system, seen in Figure 3, contains many advancements to its predecessor. One of the primary improvements is the use of direct digital synthesizers (DDS) to generate and modulate sine wave signals rather than a line stretcher/phase shifter circuit. Additionally, a microcontroller and field programmable gate array (FPGA) system are used to dynamically control system parameters. A computer also connects to the microcontroller via a terminal to control and view data from the system. These modifications have made the system more stable, easier to operate, and more sensitive to small phase changes, and some of the major components can be seen in TABLE 2.

The phase measurement method uses an ultrasonic transducer in pulse-echo mode of operation. The twin DDSs generate sine waves at the frequency, amplitude, and phase given by the user via the computer terminal and microcontroller. Then, the transmitted signal leaves the ultrasonic transducer and interrogates the bonded joint before being received back by the transducer. Meanwhile, the other generated sine wave, the reference signal, is passed directly to a phase detector circuit for later comparison.

TABLE 2: MAJOR COMPONENTS USED IN CFPPLL INSTRUMENT

Component	***Model***
Microcontroller	ATMEL ATmega644
FPGA	FreeForm/104 board with Xilinx Spartan 3E FPGA
DDS	Analog Devices AD9912
Transducer	¼" Diameter 10 MHz, Olympus V112-RM
Temp. Controller	Omega CN7823

Since piezoelectric transduction has low efficiency and some energy is lost to scattering and transmission, the received ultrasonic signal has an extremely low amplitude compared to the original electromagnetic wave generated by the DDS. After amplification, the received signal is filtered to remove undesired signals and noise. The system is currently designed to operate around a center frequency of 10 MHz. Accordingly, the filtering circuit has a -3 dB bandwidth of ~1.7 MHz, operating from 9.1 MHz to 10.8 MHz. Additionally, a 10 MHz broadband transducer is typically used for experiments, which has its own band-pass response which is more broadband than the filtering circuit, providing only a small change to the system bandwidth.

After filtering, the received signal is passed to the phase detector. The phase detector circuit outputs a voltage dependent on the phase difference between the reference and transmitted signals, using quadrature or $\pi/2$ offset as the 0 V reference. Rather than directly measuring the phase difference between the two signals, the microcontroller attempts to correct any phase difference by changing the phase of the transmitted signal until the waves are in quadrature again. As the transmitted and reference waves are synchronized in phase when generated, the absolute phase difference between reference and transmitted paths can be measured. In the current system, the absolute maximum phase and frequency resolution are set by the DDSs used. The DDSs have 14 bits of phase resolution and 48 bits of frequency resolution resulting in a minimum phase shift of $\sim 0.0220° = 3.835 \times 10^{-4}\ rad$ and frequency shift of $\sim 3.55\ \mu Hz$.

When the phase difference is "locked" to quadrature by the microcontroller, the phase adjustment needed to reach quadrature is sent to the computer via a serial interface to the terminal. After the phase adjustment has stabilized, the net phase change is simply the inverse of the absolute phase shift of the bonded structure.

For phase shift with respect to thermal stress measurements, the phase difference remains "locked" in quadrature so as to track the phase shift over time as temperature is changed. A custom-built environmental chamber with measured temperature stability to less than $\pm 0.01°C$ over the course of an hour was used.

Modeling of Phase vs. Temperature of Ultrasonic Reflection

To see how phase versus temperature measurements can be used to quantitatively determine adhesion quality, consider Al 6061 bonded to an epoxy adhesive film of thickness 76 μm. The parameters used in the model can be found in TABLE 3, where the acoustic impedance is found from the equation, $Z = \rho c$. The parameters used were either found via laboratory experiments or estimation from typical values in the literature. This model assumed a temperature change from $20°C$ to $25°C$. With such a small temperature change, the interfacial stiffness constants, K_1 and K_2 were assumed constant, as discussed in the "Interfacial Stiffness Measurement Approach" section.

TABLE 3: PARAMETERS USED TO MODEL ALUMINUM 6061-EPOXY FILM SLJ

Parameter	***Adherents***	***Adhesive***
Density, ρ	$2681\ kg/m^3$	$2530\ kg/m^3$
Sound Velocity, c	$6.428\ mm/\mu s$	$2.149\ mm/\mu s$
Frequency, f	$10\ MHz$	$10\ MHz$
Thickness, L	$6.549\ mm$	$76.2\ \mu m$

A plot of the expected phase shift derivative with respect to temperature for different interfacial stiffness values of each interface can be seen in Figure 4. As previously mentioned, good adhesive interfaces have high interfacial stiffness constants, while poor interfaces have low interfacial stiffness constants. Note that the phase shift between high and low K_1 for a given K_2 is greater than the phase shift between high and low K_2 for a given value of K_1. This implies phase versus temperature measurements will be more sensitive to the quality of the first interface in a SLJ structure. Thus, reflection measurements from the reverse side or from the lower adherent may be necessary to gain more information about the second interface in the structure. From Figure 4, there is $\sim 0.45\ °/°C$ difference between both good and both bad interfaces. The total temperature change can be raised to increase sensitivity to $d\phi/dT$. Thus, a $5°C$ change will result in a $\sim 2.25°$ phase difference between both interfaces being good and being bad, while a $10°C$ change will induce a $\sim 4.5°$ phase difference between both good and bad interfaces. With $0.022°$ phase resolution, this phase versus temperature technique should be able to quantitatively measure adhesion quality of imperfect interfaces.

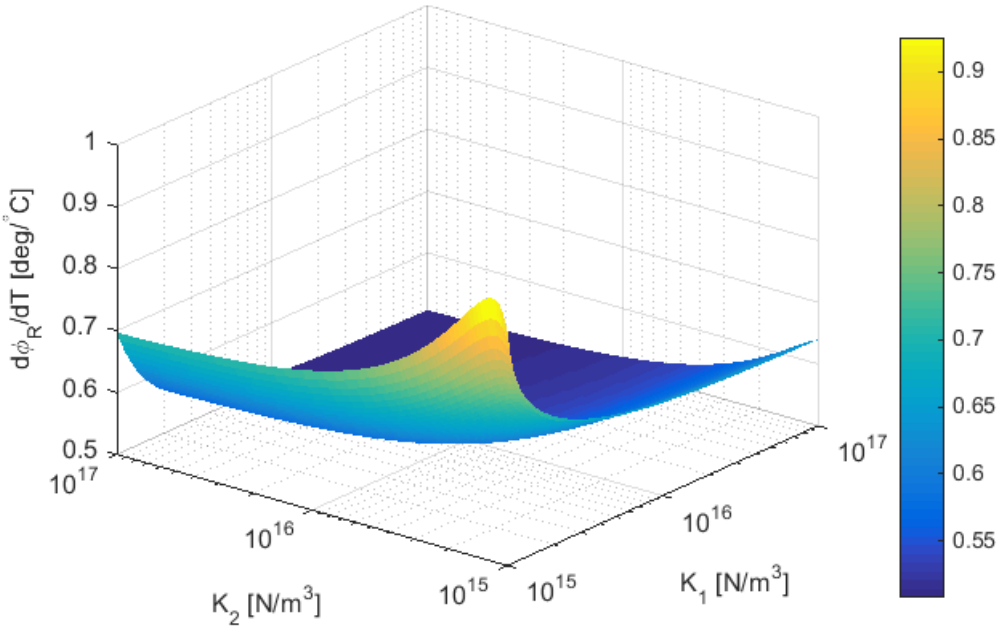

Figure 4: Modelled $d\phi_R/dT$ of Al 6061-epoxy film SLJ over a $20°C$ to $25°C$ temperature change

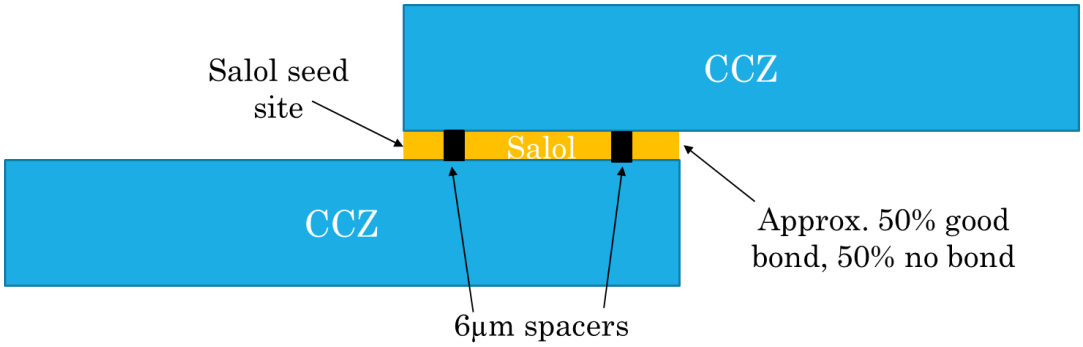

Figure 5: CCZ-salol bonded joint

Initial Results from Ultrasonic Phase vs. Temperature Measurements

To initially test the CFPPLL ultrasonic phase measurement method, a bonded specimen was created using a glass-ceramic from Ohara known as CLEARCERAM-Z (CCZ). A depiction of the bonded joint can be seen in Figure 5. This material was chosen for its low thermal expansion properties, which could minimize the effect of adherent thermal expansion on phase shift with respect to temperature measurements. The adhesive used for this specimen was the chemical, phenyl salicylate, also known as "salol". Salol was chosen for ease of creation of bonded specimens due to its low melting point ($\sim 40°C$) and for reusability of adherents after bond destruction with simple cleaning.

The CCZ-salol bonded joint was formed by melting salol, applying some to a CCZ substrate, and applying the top adherent in place. Next, a small amount of crystallized salol was placed along the edges of the sample to seed salol crystallization during cooling. Bondline thickness was controlled with four $\sim 6\mu m$ metal film pieces used as spacers in the corners of the specimen. Pressure was applied to the joint during salol cooling to maintain uniform thickness. Liquid salol was purposefully not placed on one half of the joint in an attempt to created voided and porous regions as the salol spread across the region with pressure applied.

After salol cooling, the bonded joint was examined visually for defects. As planned, approximately half of the joint appeared visually to be well-bonded without noticeable pores or voids. However, the other half of the joint had obvious regions of voids and pores. These voided and porous areas were purposefully created to allow for testing on both good and poorly bonded regions.

Ultrasonic phase measurements were carried out on different regions of the specimen while in a custom-built temperature-controlled environmental chamber, as shown in Figure 6. The chamber was programmed to start at $\sim 20°C$ and ramp up in $0.5°C$, 20 minute long steps until $25°C$ was reached. At each intermediate step, temperature was held constant for 85 minutes to ensure the specimen reached thermal equilibrium, as seen by both the temperature and phase signals flattening off near the end of each "soak" step.

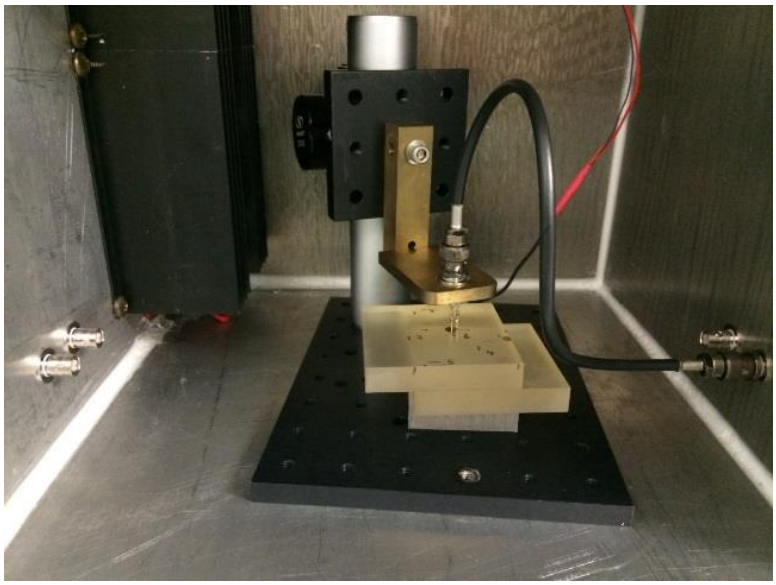

Figure 6: Image of CCZ-salol bonded specimen in environmental chamber with bare-element ultrasonic transducer.

A thermistor adhered to the side of the specimen was connected to the CFPPLL circuit to track temperature over time, as shown in Figure 7. Figure 7 also shows an example of how the phase shift in the bonded specimen varies over time while the specimen is heated. As can be seen, the phase shift tracks very well with the temperature change, as should be expected since they should have a linear relationship. As CCZ has very low thermal expansion ($0.0 \pm 1.0 \times 10^{-7}/°C$), the phase shift in the CCZ is negative for increasing temperature due to the sound velocity increasing for increasing temperature, an effect seen in some glasses but not usually in other materials such as metals. For measurement, one phase and temperature data point was taken at the end of a "soak" cycle after the structure had reached thermal equilibrium. Then, linear fits were applied to the temperature versus phase shift curves to obtain $d\phi/dT$ values. Figure 8 shows the results from phase measurement versus temperature measurements at six locations on the CCZ-salol structure. These locations were picked out visually, as the glass was transparent enough to view macroscopic bonding issues such as large voids or porosity. Two tests were carried out at each location and the resulting $d\phi/dT$ value comes from the linear fit of the phase versus temperature curve.

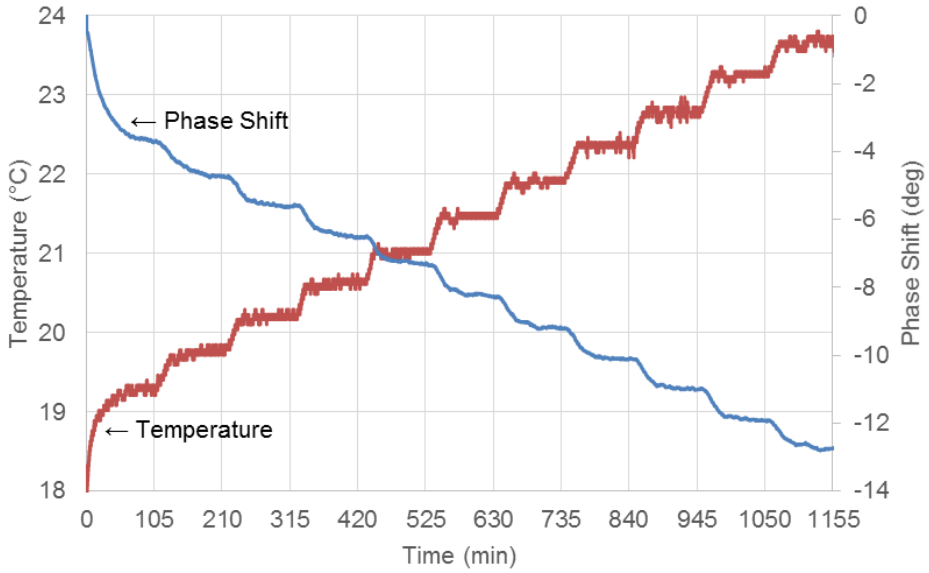

Figure 7: Phase shift and temperature vs. time for CCZ-salol bonded specimen while heating

First, $d\phi/dT$ was measured on a bare, unbonded region of the CCZ to have a reference representative of a complete disbond. Next, tests were done on the edge of the bonded area of the sample, as pointed out in Figure 5, so that approximately half the tested region was well bonded and half was completely disbonded. Tests were also performed on a region that appeared to have a large void in the salol, as well as two different locations appearing to have porosity. Finally, tests were performed on a bonded region that visually appeared well-bonded. From the $d\phi/dT$ results, it seems like the phase measurement method was indeed sensitive to different adhesion quality and adhesive defects. There exists strong correlation between measured $d\phi/dT$ and observable bonding defects in the initial test specimen.

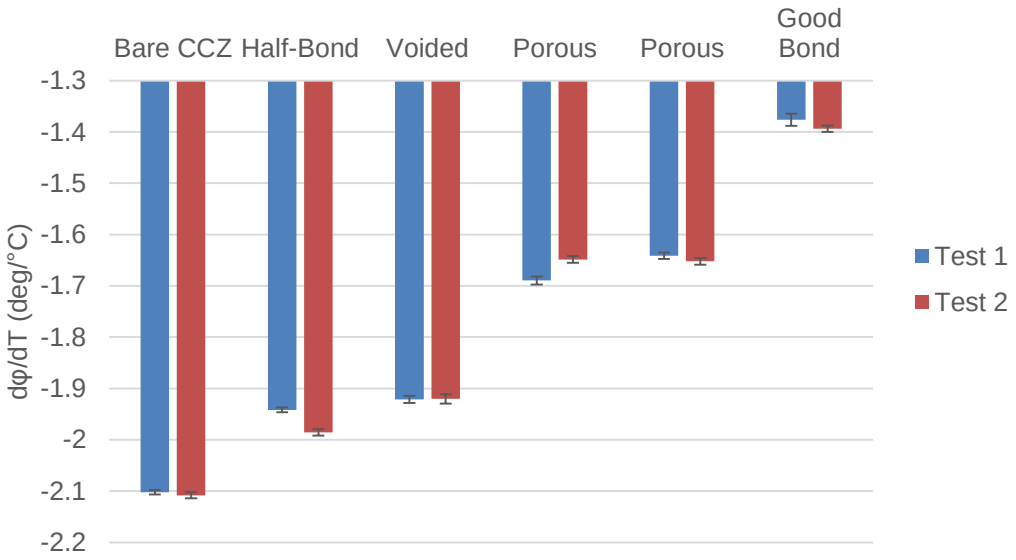

Figure 8: $d\phi/dT$ measurements from different locations on CCZ-Salol-CCZ specimen

CONCLUSIONS

The development of the CFPPLL-based instrument described here shows great potential to identify previously difficult-to-detect adhesive bond defects and potential for nondestructively quantifying adhesive bond strength. After interrogating a bonded structure with an ultrasonic wave, this method can precisely measure the phase response of a bonded interface due to thermal stress. Phase measurements should allow for high resolution measurements of adhesion properties, while still using conventional ultrasonic transducers and frequency ranges.

Furthermore, theoretical modeling shows the potential of phase measurements to measure small differences in interfacial stiffness, the key parameter to determining adhesion strength in bonded structures. Also, initial laboratory experiments show promising results in detecting reduced adhesion strength. More experiments and modeling on both metal and composite joints are being performed to quantitatively show the phase measurement method's capabilities. Previous NDE and ultrasonic methods have displayed an ability to characterize adhesive bonding defects but have struggled with quantifying adhesion strength and detecting kissing bonds. Thus, this ultrasonic phase measurement method has the potential to allow more widespread use of adhesives and advanced composites in aerospace and automotive design and repair through bond strength assurance.

REFERENCES

[1] A. I. Lavrentyev and S. I. Rokhlin, "Determination of elastic moduli, density, attenuation, and thickness of a layer using ultrasonic spectroscopy at two angles," *Journal of the Acousical Society of America*, vol. 102, no. 6, pp. 3467-3477, 1997.

[2] S. I. Rokhlin, L. Wang, B. Xie, V. A. Yakovlev and L. Adler, "Modulated angle beam ultrasonic spectroscopy for evaluation of imperfect interfaces and adhesive bonds," *Ultrasonics*, vol. 42, pp. 1037-1047, 2004.

[3] P. B. Nagy, "Ultrasonic detection of kissing bonds at adhesive interfaces," *Journal of Adhesion Science and Technology*, vol. 5, no. 8, pp. 619-630, 1991.

[4] E. P. Papadakis, "Ultrasonic phase velocity by the pulse-echo-overlap method incorporating diffraction phase corrections," *Journal of the Acoustical Society of America*, vol. 42, no. 5, pp. 1045-1051, 1967.

[5] J. Krolikowski and J. Szczepek, "Phase shift of the reflection coefficient of ultrasonic waves in the study of the contact interface," *Wear*, vol. 157, pp. 51-64, 1992.

[6] K. Milne, P. Cawley, P. B. Nagy, D. C. Wright and A. Dunhill, "Ultrasonic non-destructive evaluation of titanium diffusion bonds," *Journal of Nondestructive Evaluation*, vol. 30, pp. 225-236, 2011.

[7] E. Escobar-Ruiz, D. C. Wright, I. J. Collison, P. Cawley and P. B. Nagy, "Reflection phase measurements for ultrasonic NDE of titanium diffusion bonds," *Journal of Nondestructive Evaluation*, vol. 33, pp. 535-546, 2014.

[8] H. G. Tattersall, "The ultrasonic pulse-echo technique as applied to adhesion testing," *Journal of Physics D: Applied Physics*, vol. 6, pp. 819-832, 1973.

[9] J.-M. Baik and R. B. Thompson, "Ultrasonic scattering from imperfect interfaces: A quasi-static model," *Journal of Nondestructive Evaluation*, vol. 4, no. 3/4, pp. 177-196, 1984.

[10] T. Reddyhoff, S. Kasolang, R. S. Dwyer-Joyce and B. W. Drinkwater, "The Phase Shift of an Ultrasonic Pulse at an Oil Layer and Determination of Film Thickness," *Proceedings of the Institution of Mechanical Engineers, Part J: Journal of Engineering Tribology*, vol. 219, no. 6, pp. 387-400, 2005.

[11] J. H. Cantrell, "Determination of absolute bond strength from hydroxyl groups at oxidized aluminum-epoxy interfaces by angle beam ultrasonic spectroscopy," *Journal of Applied Physics*, vol. 96, no. 7, pp. 3775-3781, 2004.

[12] J. H. Cantrell, "Hydrogen bonds, interfacial stiffness moduli, and the interlaminar shear strength of carbon fiber-epoxy matrix composites," *AIP Advances*, vol. 5, p. 037125, 2015.

[13] A. I. Lavrentyev and S. I. Rokhlin, "Ultrasonic spectroscopy of imperfect contact interfaces between a layer and two solids," *Journal of the Acoustical Society of America*, vol. 103, no. 2, pp. 657-664, 1998.

[14] M. Schoenberg, "Elastic wave behavior across linear slip interfaces," *Journal of Acoustical Society of America*, vol. 68, no. 5, pp. 1516-1521, 1980.

[15] W. T. Yost, J. H. Cantrell and P. W. Kushnick, "Fundamental aspects of pulse phase-locked loop technology-based methods for measurement of ultrasonic velocity," *Journal of the Acoustical Society of America,* vol. 91, no. 3, pp. 1456-1468, 1992.